A Temperature Non-Equilibrium Reactive Model for Detonation Hydrodynamics

William Morin, James G. McDonald and Matei I. Radulescu
University of Ottawa
Ottawa, ON, Canada

1 Introduction

Detonation waves in gases exhibit a distinctive cellular structure that controls the overall rate of energy release. The cellular structure consists of repeated triple shock reflections driven by the coupling of reactivity to shocks inducing the reactions: the Mach and transverse shocks [1]. Owing to the wide variations in temperature, the reaction rates can be very large behind the stronger parts of the front. These local hotspot regions with enhanced reactivity are believed to control the initiation and propagation limits of detonations. Recently, numerical evidence by Murugesan [2] using molecular dynamics showed that reactivity may couple with the non-equilibrium structure of shock waves. Furthermore, they observed reactions evolving faster than predicted by the assumption of local equilibrium reaction rate. They attributed these enhancements to the Zel'dovich mechanisms of super-collisions inside the shock structure [3]. Inside the shock, the translational temperature in the direction of the shock propagation is higher than the equilibrium one. This can lead to local super-collisions enhancing the reactivity. The super-collision mechanism was further studied by Jayaraman et al. [4] via molecular dynamics of inert shocks, who clearly established the origin of the enhanced collision amplitude inside the shock. The question that arise is: can this effect be modelled quantitatively using kinetic theory in a framework conducive to a hydrodynamic model for the detonation fluid mechanics. The present study reports our progress in answering this important question. In this work, we use a mesoscale model based on moments of the Boltzmann equation. This allows us to accurately model the relaxation process of translational temperature associated with shocks. A new reactive kinetic model accounting for multiple translational temperatures is also formulated.

This extended abstract is organized as follows. We briefly review the moment method for solving Boltzmann's equation We then provide our new closure of the reactivity in the presence different translational temperatures. The model is used to examine the role of non-equilibrium in the problem of shock to detonation transition, which was studied using molecular dynamics by Murugesan [2]. We also report an evaluation of the non-equilibrium structure of triple points, and will communicate the reactive coupling at the Colloquium.

2 Kinetic Theory and The Reactive Diatomic 10-Moment Model

Kinetic theory of gases commonly describes the motion of classical gas particles through a velocity distribution function in phase space. The time evolution of this distribution function is governed by

Correspondence to: wmorin@uottawa.ca

the Boltzmann equation. As the direct discretization of the kinetic equation if prohibitively expensive, moment closure was found to be a promising method for simplifying kinetic equations into fluid models [5–10]. Moment-closure techniques use a probability distribution function, $\mathcal{F}(x_i, v_i, \omega, t)$, describing the phase-space particle density. In most cases, only a small number of macroscopic properties are of interest and not all the information contained in the distribution function is necessary. These macroscopic properties can be obtained by taking moments of the distribution function. The following are examples of moments yielding macroscopic properties of interest:

$$\rho = \int m\mathcal{F}\,\mathrm{d}v_i = \langle m\mathcal{F}\rangle\ , \quad \rho u_i = \langle m v_i \mathcal{F}\rangle\ , \qquad P_{ij} = \langle m c_i c_j \mathcal{F}\rangle\ , \qquad Q_{ijk} = \langle m c_i c_j c_k \mathcal{F}\rangle\ .$$

The bulk velocity is given by u_i, while c_i represents the random velocity, which is expressed as $c_i = v_i - u_i$. The variables ρ, P_{ij}, and Q_{ijk} are the mass density, the the generalized pressure tensor, and the heat flux respectively. The time evolution of the distribution function is described by the Boltzmann equation,

$$\frac{\partial \mathcal{F}}{\partial t} + v_i \frac{\partial \mathcal{F}}{\partial x_i} + \frac{\partial\left(a_i \mathcal{F}\right)}{\partial v_i} = \frac{\delta \mathcal{F}}{\delta t}\,. \tag{1}$$

The second term of Eq. (1) represents the convective contribution to the time evolution. In this work the acceleration is assumed to be zero. The right-hand side of the equation represents the effects of inter-particle collisions on the distribution function. In order to obtain a set of PDEs describing the evolution of the properties of interest, velocity moments of the Boltzmann equation are taken. Unfortunately, this method does not lead to a closed set of equations, since the time evolution of a given moment always depend on the spacial divergence of a moment that is one order higher. One method to close the system of equations is to assume a form for $\mathcal{F}$. In the present work, a diatomic extansion of the 10-moment Gaussian closure is used. The corresponding moment equations can be obained assuming that the distribution function is given by,

$$\mathcal{G}_D(x_i, v_i, \omega, t) = \frac{n^2 I}{(2\pi)^{5/2}(\det\Theta)^{1/2} p}\left(\frac{T}{T_{rot}}\right) e^{(-\frac{1}{2}\Theta_{ij}^{-1} c_i c_j)} e^{(-\frac{1}{2} R\omega^2)}\,, \tag{2}$$

where $\Theta_{ij} = P_{ij}/\rho$ is the temperature tensor, I is the moment of inertial about the molecule axis of rotation, ω is the angular velocity and

$$R = \frac{I}{\kappa T_{rot}} = \frac{nI}{p}\left(\frac{T}{T_{rot}}\right)\,. \tag{3}$$

This results in a set of eleven partial-differential equations describing the transport of the macroscopic quantities ρ, u_i, P_{ij} and E_{rot} (the rotational energy). Reactions are modeled as a single-step process using a progress variable, λ, tracking the mass ration of reactant, effectively adding one equation to the system. The moment system can be written as

$$\frac{\partial \rho}{\partial t} + \frac{\partial}{\partial x_k}\left(\rho u_k\right) = 0\,, \tag{4}$$

$$\frac{\partial}{\partial t}(\rho u_i) + \frac{\partial}{\partial x_k}(\rho u_i u_k + P_{ik}) = 0\,, \tag{5}$$

$$\begin{aligned}\frac{\partial}{\partial t}\left(P_{ij} + \rho u_i u_j\right) + \frac{\partial}{\partial x_k}\left(\rho u_i u_j u_k + u_i P_{jk} + u_j P_{ik} + u_k P_{ij}\right) \\ = -\frac{P_{ij} - \frac{1}{3}P_{kk}\delta_{ij}}{\tau_t} - \frac{(\frac{1}{3}P_{kk} - p)\delta_{ij}}{\tau_{rot}} + \frac{(\rho\lambda q_{kk}\delta_{ij})}{\tau_r}\,,\end{aligned} \tag{6}$$

$$\frac{\partial}{\partial t}(E_{rot}) + \frac{\partial}{\partial x_k}(u_k E_{rot}) = -\frac{(E_{rot} - p)}{\tau_{rot}} + \frac{(\rho\lambda q_{rot})}{\tau_r} \,. \tag{7}$$

$$\frac{\partial}{\partial t}(\rho\lambda) + \frac{\partial}{\partial x_k}(\rho u_k \lambda) = -\frac{(\rho\lambda)}{\tau_r} \,, \tag{8}$$

where, q represent the heat release of each energy mode and τ_r is the reaction time computed as the bimolecular collision rate multiplied by the fraction of collisions with sufficient energy to react. It is important to note that the resulting equation assumes a rigid "dumbbell" molecular model. Therefore, no vibrational energy is considered. The relaxation times τ_t and τ_{rot} are modeled following Hittinger [11].

3 A New Reaction Rate Model

Accurate modelling of both the collision and reaction rates is paramount. Traditional methods for the estimation of these quantities assume thermodynamic equilibrium greatly limiting their validity in situations where non-equilibrium effects are important. In this work, new models for both the collision and reaction rate are introduced and tested using one-dimensional shock to detonation transition calculations. This model takes into account temperature anisotropy by assuming a 10-moment distribution function for the particle velocities. It is derived following the classical result from Vincenti and Kruger [12]. Assuming indistinguishable particles, the new bimolecular collision rate model is given by ,

$$Z_{\mathcal{G}} = \frac{d^2 n^2}{2\sqrt{\pi}} \Theta^* \,, \tag{9}$$

where Θ^* is defined as the following surface integral,

$$\Theta^* = \int_0^{2\pi} \int_0^{\pi} \sqrt{T_{xx} \sin^2\theta_g \cos^2\phi_g + T_{yy} \sin^2\theta_g \sin^2\phi_g + T_{zz} \cos^2\theta_g} \sin\theta \mathrm{d}\theta \, \mathrm{d}\phi \ , \tag{10}$$

In the equilibrium limit, where $T_{xx} = T_{yy} = T_{zz}$ Eq. (9) recovers the classical equilibrium bimolecular collision rate,

$$Z_{\mathcal{M}} = \frac{d^2 n^2}{2} \sqrt{\frac{8\pi k \hat{T}}{m^*_{AB}}} \,, \tag{11}$$

where $\hat{T}$ is the equilibrium temperature in Kelvin, k is Boltzmann's constant, m^*_{AB} is the reduced mass, which is $m/2$ when equal masses are considered. The fraction of collisions with enough energy to yield reaction is found as,

$$\frac{Z_{E_a}}{Z_{\mathcal{G}}} = \frac{\Omega^*}{\Theta^* \sqrt{T_{xx} T_{yy} T_{zz}}} \,, \tag{12}$$

where E_a is the activation energy. The term Ω^* is given by,

$$\Omega^* = \int_0^{2\pi} \int_0^{\pi} \frac{\exp\left[E_a \left(\frac{\sin^2\theta_g \cos^2\phi_g}{T_{xx}} + \frac{\sin^2\theta_g \sin^2\phi_g}{T_{yy}} + \frac{\cos^2\theta_g}{T_{zz}}\right)\right]}{\left(\frac{\sin^2\theta_g \cos^2\phi_g}{T_{xx}} + \frac{\sin^2\theta_g \sin^2\phi_g}{T_{yy}} + \frac{\cos^2\theta_g}{T_{zz}}\right)^2} \sin\theta \mathrm{d}\theta \, \mathrm{d}\phi \ , \tag{13}$$

which again recovers the well-known equilibrium model,

$$\frac{Z_{E_a}}{Z_{\mathcal{M}}} = \exp\left[\frac{-E_a}{T}\right] \,, \tag{14}$$

in the case of no temperature anisotropy. Figure 1 shows one-dimensional shock to detonation transition calculations as predicted by the one-step reactive Euler equations and the new reactive 10-moment

model. The governing equations are non-dimensionalised using the unshocked state. All cases are run with the normalized activation energy held constant at $E_a = 50$. The calculations are run using a first-order Godunov-type finite volume scheme on a grid of 10000 cells. The results of the first case (Ma = 2), indicates that neither models predicts a transition to detonation on the observation time scales. Conversely, for the third case (Ma = 8), both models predict an overdriven detonation with similar reaction rates. The Euler model shows a slightly faster reaction rate due to its inherently larger collision rate. However, the important difference can be observed for the second case (Ma = 4.5), where the reactive Euler system yields considerably slower reactions. The 10-moment model predict a stronger wave with almost twice the overpressure. The ability of the new reaction model to consider the non-equilibrium effect across the shock highlights the effect of translational temperatures on detonation hydrodynamics.

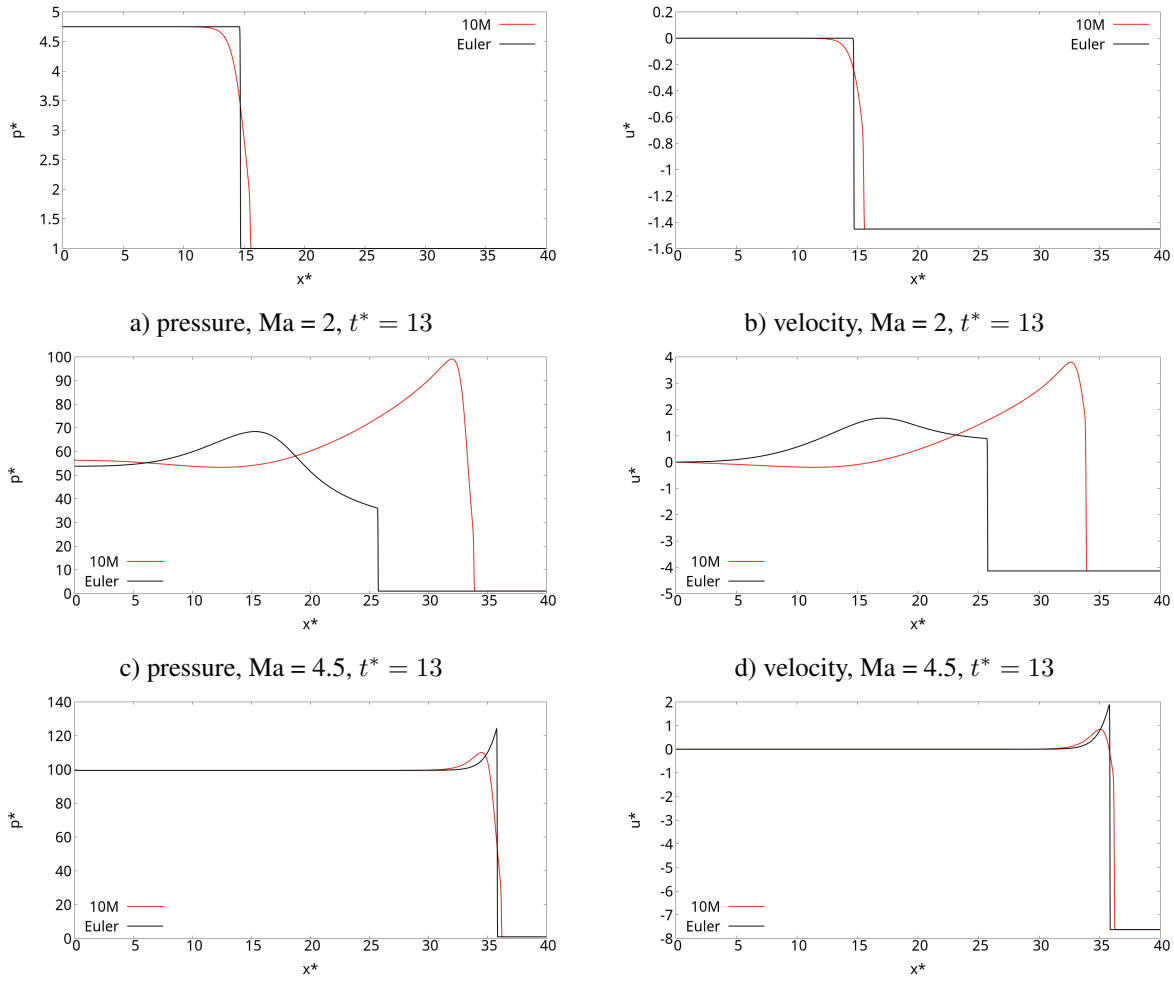

a) pressure, Ma = 2, $t^* = 13$

b) velocity, Ma = 2, $t^* = 13$

c) pressure, Ma = 4.5, $t^* = 13$

d) velocity, Ma = 4.5, $t^* = 13$

e) pressure, Ma = 8, $t^* = 7$

f) velocity, Ma = 8, $t^* = 7$

Figure 1: Shock to detonation transition calculations using the 10-moments model for Ma = 2, Ma = 4.5, Ma = 8 and $E_a = 50$. The left column shows the non-dimensional pressure, p^* and the right column shows the normalized velocity, u^* as function of distance.

4 The Inert Triple Shock Problem

The inert triple shock reflection problem is studied numerically using the diatomic 10-moment model. All calculations are computed using a discontinuous-Galerkin-Hancock scheme, ensuring third-order accuracy in both space and time. The simulations are run in parallel using adaptive mesh refinement to accurately capture the solutions' structure. The refinement criteria is adjusted such that a minimum of 75 grid points are present across the shock waves at any given time to ensure that the shock wave non-equilibrium structure is capture accuratly. The system of equations are non-dimensionalised by,

$$\rho^* = \rho/\rho_{\text{ref}}, \quad p^* = p/p_{\text{ref}}, \quad u_i* = u_i/\sqrt{p_{\text{ref}}/\rho_{\text{ref}}}, \quad x^* = x/\lambda_{\text{ref}}, \quad y^* = y/\lambda_{\text{ref}},$$
$$t^* = t\,\sqrt{p_{\text{ref}}/\rho_{\text{ref}}}/\lambda_{\text{ref}} \quad \text{and} \quad \mu^* = \mu/\sqrt{p_{\text{ref}}\rho_{\text{ref}}}\,\lambda_{\text{ref}}\,.$$

The reference state is chosen to be the unshocked state with mean free path,

$$\lambda_{\text{ref}} = \frac{RT_{\text{ref}}}{\sqrt{2}\pi d^2 N_A p_{\text{ref}}}\,, \tag{15}$$

following the derivation for a gas at equilibrium by Vincenti and Kruger [12]. The constant N_A is Avogadro's number, d is the molecular size and R is the gas constant. Since the calculation are run for air, the molecular size is set to $d = 3.4 \times 10^{-10}$ leading to a mean free path of, $\lambda_{\text{ref}} = 7.7 \times 10^{-8}$ at atmospheric conditions. The non-dimensional viscosities are held constant at $\mu^* = 0.83$ and $\mu_B = 3\mu = 2.49$. The initial conditions were calculated using the ideal three-shock solution [1,2] with an normal mach shock of strength Ma = 8.7 and an mach shock angle of 153° between the incident and Mach shocks. The initial conditions are depicted in Figure 2. The calculations are run on a rectangular domain of size 240 by 100 mean free paths using an in-house code. The density profile of both the viscous and inviscid reflections is shown in Fig. 3 and Fig. 4 at a time $t^* = 17$. The double Mach reflection formed on the right is seen at $x^* \approx 60$, and the regular reflection formed on the left is seen at $x^* \approx -115$. The double Mach reflection propagating through the unshocked gas arises from the reflection of the original Mach stem with the bottom wall. One can observe small evidence of Kelvin–Helmholtz instabilities along the original contact surface. The contact surface jets towards the Mach stem along the bottom wall is also clearly visible in both simulations. Figure 5, shows both the density and translational temperature, T^*_{xx}, profiles of the newly formed triple point at the Mach reflection. The computational mesh is also visible on the density profile, highlighting the high resolution used in the computations. One can observe that the temperature anisotropy is maximum at the triple point location. Based on the one-dimensional calculations shown above, this temperature hot-spot could greatly influence the chemical kinetics.

5 Concluding Remarks

In light of the findings presented in this abstract, reactive triple shock reflection calculations using the new temperature non-equilibrium reactive model will be presented at the 30th international colloquium on the dynamics of explosions and reactive systems. These calculations are expected to highlight the importance of non-equilibrium effects on detonation dynamics.

6 Acknowledgment

The authors acknowledge the financial support provided by AFOSR grant FA9550-23-1-0214, with Dr. Chiping Li as program monitor.

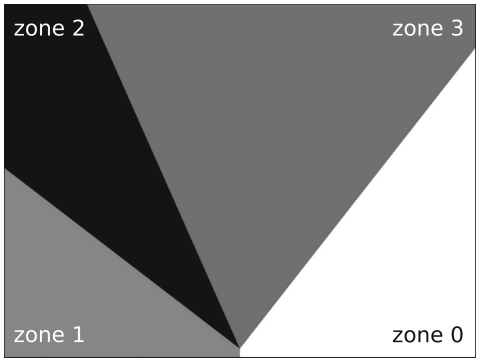

	zone 0	zone 1	zone 2	zone 3
ρ	1	5.465	7.229	5.628
u_x	-8.457	-1.547	-2.079	-0.915
u_y	0	0	-1	-3.84
p	1	59.433	88.138	88.138

Figure 2: Triple Point Initial Conditions

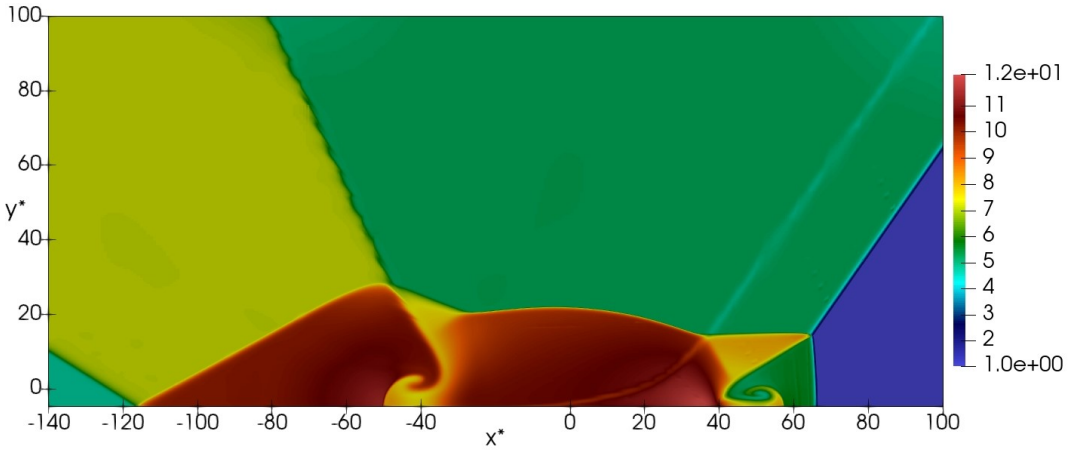

Figure 3: Density field of a triple shock reflection as predicted by the 10-moment model at $t^* = 17$.

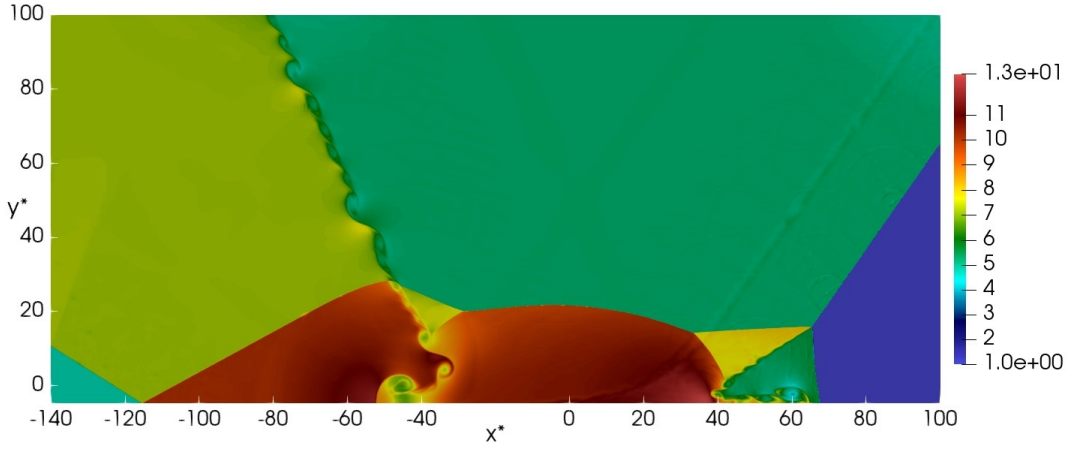

Figure 4: Density field of a triple shock reflection as predicted by the Euler model at $t^* = 17$.

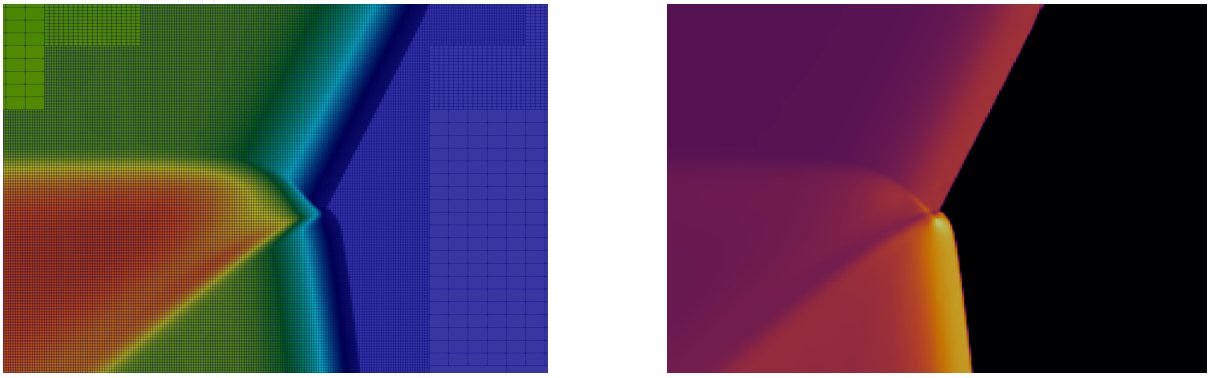

a) ρ^*, at $t^* = 17$ b) T^*_{xx}, at $t^* = 17$

Figure 5: Zoomed plots of the triple point: density (on the left) and the translational temperature T_{xx} (on the right).

References

[1] W. Fickett and W. C. Davis. Detonation: theory and experiment. 2012.

[2] R. Murugesan. *Translational Non-Equilibrium Effects in Reactive Dynamics of Detonations*. PhD thesis, Université d'Ottawa/University of Ottawa, 2023.

[3] B. I. A. kovlevich Zeldovich, D. Wallace Hayes, and Raizer. *Physics of schock waves and high-temperature hydrodynamic phenomena*. Academic Press, 1966.

[4] A. S. Jayaraman, E. S. Genter, W. Dong, and H. Wang. Collision enhancement in shocks and its implication on gas-phase detonations: A molecular dynamics and gas-kinetic theory study. *Proceedings of the Combustion Institute*, 40(1-4):105741, 2024.

[5] S. L. Brown, P. L. Roe, and C. P. T. Groth. Numerical solution of a 10-moment model for nonequilibrium gasdynamics. Paper 95-1677, AIAA, June 1995.

[6] M. Torrilhon. Modeling nonequilibrium gas flow based on moment equations. *Annual review of fluid mechanics*, 48:429–458, 2016.

[7] H. Struchtrup and M. Torrilhon. H theorem, regularization, and boundary conditions for the linearized 13 moment equations. *Physical Review Letters*, 99:014502, 2007.

[8] H. Struchtrup and T. Thatcher. Bulk equations and Knudsen layers for the regularized 13 moment equations. *Continuum Mechanics and Thermodynamics*, 19:177–189, 2007.

[9] J. G. McDonald and M. Torrilhon. Affordable robust moment closures for CFD based on the maximum-entropy hierarchy. *Journal of Computational Physics*, 251:500–523, 2013.

[10] W. Morin and J. G McDonald. Development of globally hyperbolic one-dimensional moment closures based on orthogonal polynomials. *Journal of Computational Physics*, 523:113659, 2025.

[11] J. A. Hittinger. *Foundations for the Generalization of the Godunov Method to Hyperbolic Systems with Stiff Relaxation Source Terms*. PhD thesis, University of Michigan, 2000.

[12] W. G. Vincenti, C. H. Kruger, and T. Teichmann. *Introduction to physical gas dynamics*. American Institute of Physics, 1966.